Angular Dependence of Wind-Driven Sea-Surface Retroreflectance

David M. Tratt, Meng P. Chiao, and Robert T. Menzies
Jet Propulsion Laboratory, California Institute of Technology
4800 Oak Grove Drive, Pasadena, CA 91109, USA
Tel. +1-818-354-2750

Dean R. Cutten and Jeffry Rothermel
NASA Marshall Space Flight Center/National Space Science and Technology Center
320 Sparkman Drive, Huntsville, AL 35805, USA

ABSTRACT

Concurrent measurements of sea-surface retroreflectance and associated wind velocity provide insight into thermal-infrared optical phenomenology of air-sea interface processes. These results contribute to a greater understanding of radiation transfer between the atmosphere and hydrosphere, as well as improved models of wind-driven ocean surface stress applicable to other remote sensing applications.

Angular Dependence of Wind-Driven Sea-Surface Retroreflectance

David M. Tratt, Meng P. Chiao, and Robert T. Menzies
Jet Propulsion Laboratory, California Institute of Technology
4800 Oak Grove Drive, Pasadena, CA 91109, USA

Dean R. Cutten and Jeffry Rothermel
National Space Science and Technology Center, NASA Marshall Space Flight Center
320 Sparkman Drive, Huntsville, AL 35805, USA

Introduction

The effects of wind-stress on the optical properties of the ocean surface have been studied for several decades. In particular, the seminal study by Cox and Munk (1954) linking sea-surface wind field to wave slope statistics provides a phenomenology by which the sea-surface wind velocity can be estimated from direct measurement of the wave-modulated surface reflectance. A limited number of studies along these lines have been conducted using airborne (Bufton *et al.*, 1983; Hoge *et al.*, 1984; Flamant *et al.*, 1998) or spaceborne (Menzies *et al.*, 1998) lidar systems. In these instances, surface truth was provided by *in situ* ship reports or satellite microwave remote sensing instruments.

During the 1996 and 1998 deployments of the Multicenter Airborne Coherent Atmospheric Wind Sensor (MACAWS; Rothermel *et al.*, 1998a,b) airborne Doppler wind lidar measurements of sea-surface retroreflectance as a function of azimuth- and nadir-viewing angles were acquired over US coastal waters. MACAWS data products include directly measured winds, as well as calibrated backscatter/retroreflectance profiles, thus enabling comparison of the winds inferred from sea-surface retroreflectance measurements with those derived directly from the Doppler-processed line-of-sight (LOS) estimates.

This contribution is an expanded update of the preliminary results that were previously reported by Tratt *et al.* (1998).

Instrument description

MACAWS is a scanning coherent detection Doppler lidar based on CO_2 laser technology. In the airborne configuration it is a side-viewing instrument with the capability of being scanned in any direction within a ~64° full cone angle by means of a dual rotary germanium wedge scanner. Its salient operational characteristics are given in Table 1. Further details concerning instrumental parameters and performance can be found in Rothermel *et al.* (1998a,b).

PARAMETER	VALUE	
Wavelength	10.6 μm	
PRF	20 Hz	
Beam divergence	~0.3 mrad	
	1996	*1998*
Pulse energy	0.8 J	0.25 J
Pulse duration	3 μs	0.4 μs
No. of pulses averaged	3	10
LOS range resolution	300 m	150 m
LOS velocity resolution	~1 m/s	~4 m/s

Table 1. MACAWS primary instrumental operating characteristics.

Experiment description

The experiments we will describe here were conducted from the NASA DC-8 research aircraft at flight altitudes of 20000–25000 ft (~6–7.5 km). This altitude range was selected in order to provide for high signal-to-noise ratio for the ocean surface return whilst precluding the likelihood of saturating the detection system.

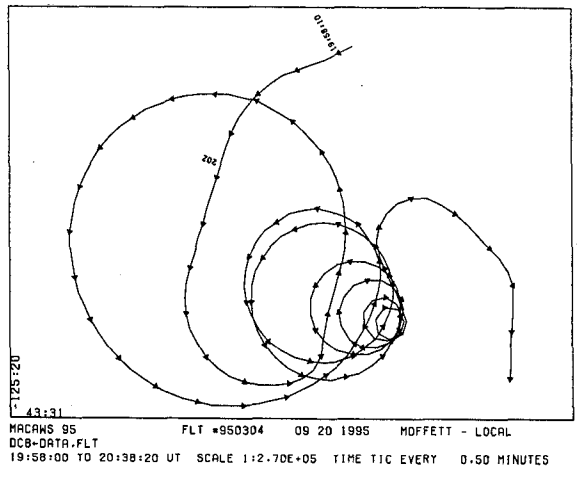

Figure 1. Example of aircraft flight track implemented for the present study.

Because the maximum beam depression angle available with the present scanner is only 30°, access to nadir viewing angles less than 60° necessitated controlled banking of the aircraft. With the scanner staring abeam of the aircraft and set for maximum depression, the DC-8 was thus flown in a series of nested circular tracks with progressively steeper bank angles in order to access a series of nadir angle viewing geometries down to $\theta = 20°$ (see Figure 1). Each circular flight track segment thus essentially represents a VAD (velocity-azimuth display) acquisition configuration.

Theory of optical scattering at the ocean surface

Due to the absorptive properties of water at the MACAWS operating wavelength, any contribution to the total reflectance due to subsurface volume scattering can be neglected, so that the retroreflectance, R, of the wind-stressed sea surface may be expressed by (Menzies *et al.*, 1998):

$$R = \frac{\rho(1-F)\sec^4\theta}{2\pi\langle s^2\rangle}\exp\left(\frac{-\tan^2\theta}{\langle s^2\rangle}\right) + \frac{FR_F\cos\theta}{\pi},$$

in which ρ is the Fresnel reflectance of seawater for normal incidence (computed using the oceanic refractive index data of Querry *et al.* [1977]) and $\langle s^2\rangle$ is the wind-driven capillary wave mean-square slope estimated according to Cox and Munk (1954). R_F is the reflectance of sea foam (proportional coverage F), which to first order may be regarded as a Lambertian scatterer (Moore *et al.*, 1998).

Whitecap reflectance is dependent on water absorption (Frouin *et al.*, 1996). Since this property is high in the thermal infrared the resulting effect on the surface reflectivity should be negligible for our situation. Indeed, the measurements of Salisbury *et al.* (1993) bear this out, indicating that foam reflectance in the 8-14 μm spectral region is similar in magnitude to that of the seawater itself. Consequently, for the present purpose we assume $R_F = \rho$.

Assuming the wind-dependent foam coverage parameterization formulated by Koepke (1984), the modeled dependence of the ocean surface retroreflectance on wind speed and nadir viewing angle, as computed using the above expression, is depicted in Figure 2. In this figure U[10] is the wind speed at 10-m altitude above the water surface and the upwind/downwind wave slope variance is assumed, i.e., $\langle s^2\rangle \approx 0.003$U[10], where U[10] is expressed in m/s (Cox and Munk, 1954).

From this display we observe that scattering at low angles derives primarily from the specular component reflected from capillary wave facets, while at the larger nadir angles the Lambertian-distributed contribution from foam dominates.

Field measurements

The experiments were conducted on June 10, 1996 during the interval 1700–1730 UTC off the northern California coast at 38.°5N latitude, 124.°0W longitude, and on Sept. 13, 1998 during the interval 2230–2310 UTC near the Bahamas at 26.°0N latitude, 78.°5W longitude. Concurrent visual observer records estimated a sea-state of 4 for the California experiment (which was characterized by abundant whitecaps) and a sea-state of 2 for the Bahamas experiment (see Table 2).

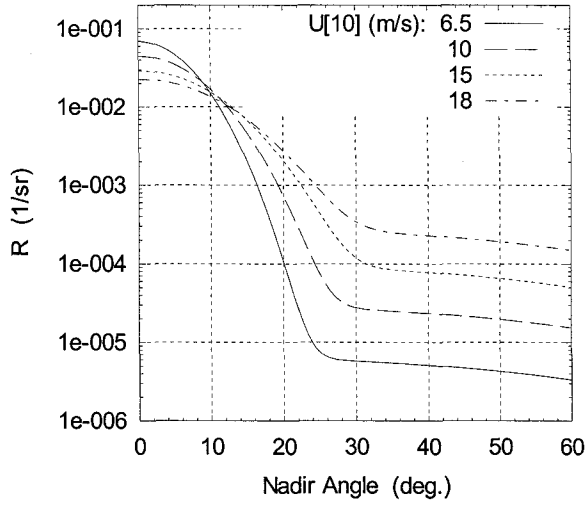

Figure 2. Modeled 10.6-μm sea-surface retroreflectance as a function of nadir angle and wind speed. The abrupt change in gradient marks the distinction between foam- and capillary wave-dominated reflectivity regimes.

SEA-STATE	DESCRIPTION	WAVE HEIGHT (m)
0	Calm-glassy	0
1	Calm-rippled	0–0.15
2	Smooth-wavelets	0.15–0.45
3	Slight	0.45–1.2
4	Moderate	1.2–2.4
5	Rough	2.4–4
6	Very rough	4–6
7	High	6–9
8	Very high	9–13.7
9	Phenomenal	>13.7

Table 2. Standard sea-state scale.

As described above, a series of circular tracks were flown above an unobscured (clear sky) ocean target at different lidar incidence angles. The resultant time series data were inverted to obtain range-resolved profiles of absolute backscatter and the sea-surface returns were integrated with respect to range in order to extract the azimuthal dependence of the surface retroreflectance. Two such azimuthal scans are represented in Figures 3 and 4, along with the associated LOS wind speeds retrieved in the marine boundary layer (MBL). In these figures the azimuth angle expresses the lidar view heading relative to due North and negative velocities are receding from the aircraft. The respective datasets have been smoothed in order to de-emphasize speckle-induced outliers arising from glint returns from the ocean surface.

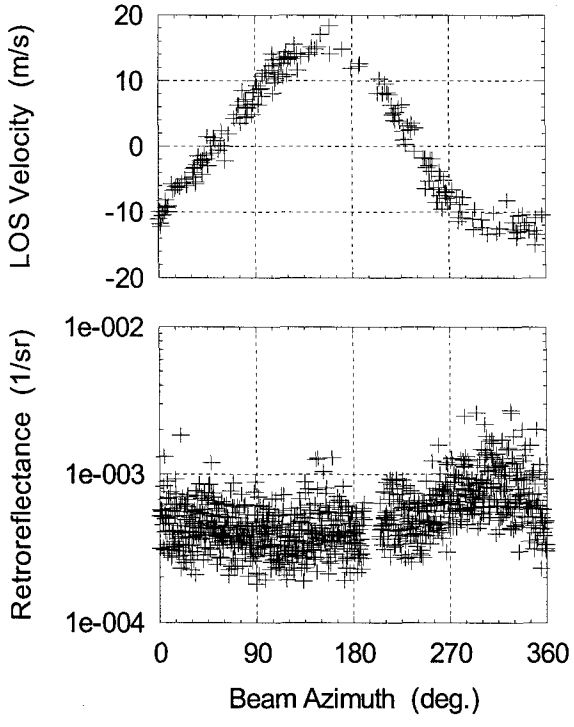

Figure 3. Azimuthal dependence of the sea-surface retroreflectance and MBL LOS velocity retrievals at a nadir viewing angle of 50°during the 1996 experiment.

The near-surface horizontal wind estimated from the LOS Doppler retrievals in Figure 3 is ~18 m/s and in Figure 4 is ~6.5 m/s. The azimuthally-resolved data presented in Figures 3 and 4 clearly reveal an asymmetric polar signature, although this feature is more pronounced in the latter dataset. In Figure 3 the comparative roughness of the ocean surface may be acting to obscure the geophysical signal, even though the surface retroreflectance itself was measured with high signal-to-noise ratio. However, the differential nature of R in the upwind and downwind directions discernable in Figure 4 is in qualitative agreement with analogous observations acquired with airborne microwave scatterometer instruments (Carswell *et al.*, 1994).

In Figure 4 the LOS wind retrievals are seen to be somewhat noisier than those depicted in Figure 3, in contrast to the clarity of the associated sea-surface retroreflectance signature. For the 1998 experiment we had operated the lidar transmitter in its short pulse mode (Post and Cupp, 1990) in order to improve the LOS spatial resolution. It is thought that under these circumstances the combination of high bank angle and short measurement time *per* angular resolution element may have precluded resolution of the LOS wind to better than 3-5 m/s, which is of the same order as the LOS wind amplitude inferred from Figure 4.

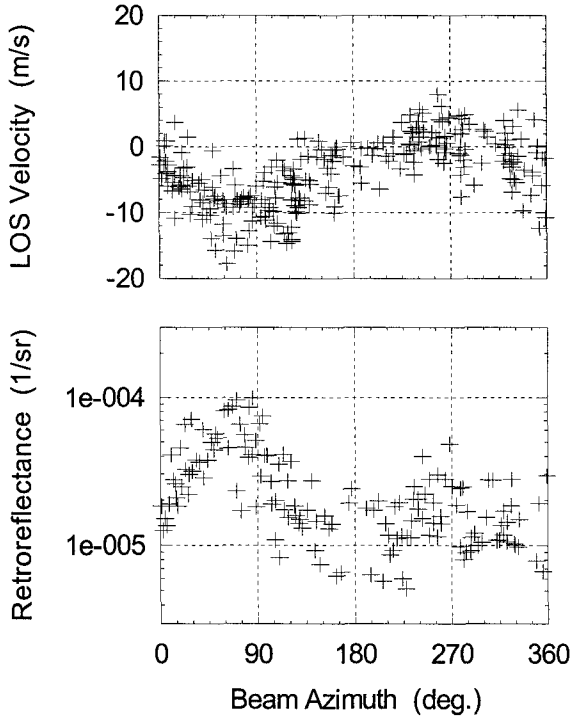

Figure 4. Azimuthal dependence of the sea-surface retroreflectance and MBL LOS velocity retrievals at a nadir viewing angle of 37°during the 1998 experiment.

The clear upwind/downwind asymmetry present in the surface retroreflectance signatures of both Figures 3 and 4 indicates that the assumption of a single-valued upwind/downwind wave slope variance parameter is invalid. Improved models of the wind-stressed ocean surface are under investigation to assist in the interpretation of these observations.

Conclusion

Measurements of the azimuthal and incidental angular dependence of sea-surface retroreflectance have been conducted with an airborne Doppler lidar operating at a wavelength of 10.6 μm in the mid-infrared. Line-of-sight wind velocity estimates also provided by the lidar data stream permit comparison of the directly measured wind field against those inferred from analysis of the surface retroreflectance data. This dataset will provide further insight into the mid-infrared optical properties of the air-sea interface, thereby contributing to a fuller understanding of radiation transfer between the ocean and atmosphere, as well as air-sea interface optical phenomenology in the thermal-infrared spectral region.

The findings reported here, while preliminary, suggest that new information relating to the physics of the air-sea interface can be gleaned from such measurements. This investigation will continue during future flights of the MACAWS instrument, using the existing data to assist in refining the experimental execution.

Acknowledgments

This work was carried out by the Jet Propulsion Laboratory, California Institute of Technology, under contract with the National Aeronautics and Space Administration (NASA), with support provided by Ramesh Kakar, Atmospheric Dynamics and Remote Sensing Program, NASA Office of Earth Science.

References

Bufton, J. L., F. E. Hoge, and R. N. Swift (1983): Airborne measurements of laser backscatter from the ocean surface. *Appl. Opt.*, **22**(17), 2603-2618.

Carswell, J. R., S. C. Carson, R. E. McIntosh, F. K. Li, G. Neumann, D. J. McLaughlin, J. C. Wilkerson, P. G. Black, and S. V. Nghiem (1994): Airborne scatterometers: Investigating ocean backscatter under low- and high-winds conditions. *Proc. IEEE*, **82**(12), 1835-1860.

Cox, C., and W. Munk (1954): Measurement of the roughness of the sea surface from photographs of the Sun's glitter. *J. Opt. Soc. Amer.*, **44**(11), 838-850.

Flamant, C., V. Trouillet, P. Chazette, and J. Pelon (1998): Wind speed dependence of atmospheric boundary layer optical properties and ocean surface reflectance as observed by airborne backscatter lidar. *J. Geophys. Res.*, **103**(C11), 25137-25158.

Frouin, R., M. Schwindling, and P. –Y. Deschamps (1996): Spectral reflectance of sea foam in the visible and near-infrared: In situ measurements and remote sensing implications. *J. Geophys. Res.*, **101**(C6), 14361-14371.

Hoge, F. E., W. B. Krabill, and R. N. Swift (1984): The reflection of airborne UV laser pulses from the ocean. *Marine Geodesy*, **8**(1-4), 313-344.

Koepke, P. (1984): Effective reflectance of oceanic whitecaps. *Appl. Opt.*, **23**(11), 1816-1824.

Menzies, R. T., D. M. Tratt, and W. H. Hunt (1998): Lidar In-space Technology Experiment measurements of sea surface directional reflectance and the link to surface wind speed. *Appl. Opt.*, **37**(24), 5550-5559.

Moore, K. D., K. J. Voss, and H. R. Gordon (1998): Spectral reflectance of whitecaps: Instrumentation, calibration, and performance in coastal waters. *J. Atmos. Oceanic Technol.*, **15**(2), 496-509.

Post, M. J., and R. E. Cupp (1990): Optimizing a pulsed Doppler lidar. *Appl. Opt.*, **29**(28), 4145-4158.

Querry, M. R., W. E. Holland, R. C. Waring, L. M. Earls, and M. D. Querry (1977): Relative reflectance and complex refractive index in the infrared for saline environmental waters. *J. Geophys. Res.*, **82**(9), 1425-1433.

Rothermel, J., D. R. Cutten, R. M. Hardesty, R. T. Menzies, J. N. Howell, S. C. Johnson, D. M. Tratt, L. D. Olivier, and R. M. Banta (1998a): The Multi-center Airborne Coherent Atmospheric Wind Sensor, MACAWS. *Bull. Amer. Meteorol. Soc.*, **79**(4), 581-599.

Rothermel, J., L. D. Olivier, R. M. Banta, R. M. Hardesty, J. N. Howell, D. R. Cutten, S. C. Johnson, R. T. Menzies, and D. M. Tratt (1998b): Remote sensing of multi-level wind fields with high-energy airborne scanning coherent Doppler lidar. *Opt. Express*, **2**(2), 40-50.

Salisbury, J. W., D. M. D'Aria, and F. F. Sabins, Jr. (1993): Thermal infrared remote sensing of crude oil slicks. *Remote Sens. Environ.*, **45**(2), 225-231.

Tratt, D. M., R. T. Menzies, and D. R. Cutten (1998): Wind-driven angular dependence of sea-surface reflectance measured with an airborne Doppler lidar. *NASA Conference Publication CP-1998-207671/Part 2*, 723-725.